Phosphorylation Controls Autoinhibition of Cytoplasmic Linker Protein-170

Ho-Sup Lee,*†‡ Yulia A. Komarova,*‡§ Elena S. Nadezhdina,*‖ Rana Anjum,¶#
John G. Peloquin,*@ Joseph M. Schober,*,** Oana Danciu,*†† Jeffrey van Haren,‡‡
Niels Galjart,‡‡ Steven P. Gygi,¶ Anna Akhmanova,‡‡ and Gary G. Borisy*§§

*Department of Cell and Molecular Biology, Northwestern University Medical School, Chicago, IL 60611;
¶Department of Cell Biology, Harvard Medical School, Boston, MA 02115; and ‡‡Department of Cell Biology,
Erasmus Medical Center, 3000 CA Rotterdam, The Netherlands

Cytoplasmic linker protein (CLIP)-170 is a microtubule (MT) plus-end-tracking protein that regulates MT dynamics and links MT plus ends to different intracellular structures. We have shown previously that intramolecular association between the N and C termini results in autoinhibition of CLIP-170, thus altering its binding to MTs and the dynactin subunit p150^{Glued} (J. Cell Biol. 2004: 166, 1003–1014). In this study, we demonstrate that conformational changes in CLIP-170 are regulated by phosphorylation that enhances the affinity between the N- and C-terminal domains. By using site-directed mutagenesis and phosphoproteomic analysis, we mapped the phosphorylation sites in the third serine-rich region of CLIP-170. A phosphorylation-deficient mutant of CLIP-170 displays an "open" conformation and a higher binding affinity for growing MT ends and p150^{Glued} as compared with nonmutated protein, whereas a phosphomimetic mutant confined to the "folded back" conformation shows decreased MT association and does not interact with p150^{Glued}. We conclude that phosphorylation regulates CLIP-170 conformational changes resulting in its autoinhibition.

INTRODUCTION

The microtubule (MT) cytoskeleton plays an essential role in numerous fundamental processes, including cell division, migration, differentiation, morphogenesis, and intracellular trafficking. A variety of accessory factors control spatial and temporal organization of the MT cytoskeleton (for reviews, see Maccioni and Cambiazo, 1995; Howard and Hyman, 2003, 2007). Among these factors is a class of proteins designated plus-end-tracking proteins (+TIPs) that specifically bind to growing MT plus ends, control MT dynamics, and transiently link MT plus ends to the actin cytoskeleton and other intracellular structures (for reviews, see Schuyler and Pellman, 2001; Akhmanova and Steinmetz, 2008).

Cytoplasmic linker protein (CLIP)-170, the first described +TIP (Perez *et al.*, 1999), was discovered as a linker between endocytic vesicles and MTs (Rickard and Kreis, 1990; Pierre *et al.*, 1992). Structural analysis of CLIP-170 shows that it is an elongated molecule dimerized through its central α-helical rod domain (Scheel *et al.*, 1999; Lansbergen *et al.*, 2004). The N-terminal region of CLIP-170 contains two MT-binding cytoskeleton-associated protein glycine-rich (CAP-Gly) domains flanked by three serine-rich stretches; the C-terminal region contains two zinc-knuckle motifs (Pierre *et al.*, 1992). Structural studies revealed the presence of positively charged basic grooves in both CAP-Gly domains involved in tubulin binding; the second CAP-Gly domain furnished with a more basic groove directly binds the acidic tail of α-tubulin (Mishima *et al.*, 2007). This CAP-Gly domain is thought to be necessary and sufficient for CLIP binding to growing MT ends in cells (Gupta *et al.*, 2009). A second mammalian CLIP, CLIP-115, has a similar structural organization but lacks the C-terminal zinc-knuckle motifs (De Zeeuw *et al.*, 1997). In contrast to the yeast homologues, which are delivered by kinesin to MT tips (Busch *et al.*, 2004; Carvalho *et al.*, 2004), CLIP-170 rapidly exchanges at the growing MT ends by recognizing composite end-binding protein 1/tubulin binding sites (Bieling *et al.*, 2008; Dragestein *et al.*, 2008).

CLIP family members are multifunctional proteins that are involved in distinct MT-dependent pathways. In general, they are "positive" regulators of MT growth (Brunner and Nurse, 2000; Komarova *et al.*, 2002; Arnal *et al.*, 2004; Carvalho *et al.*, 2004). Both mammalian CLIPs directly interact with microtubule-stabilizing factors clip-associated proteins (Akhmanova *et al.*, 2001; Mimori-Kiyosue *et al.*, 2005) and with IQGAP1, a Rac1/Cdc-42 binding factor (Fukata

et al., 2002), and may play a role in coordinating MT and actin network remodeling during cell migration.

The C-terminal zinc-knuckle motifs, which distinguish CLIP-170 from CLIP-115, directly bind to LIS1 and p150[Glued], the large subunit of dynactin complex (Coquelle *et al.*, 2002; Tai *et al.*, 2002; Goodson *et al.*, 2003; Lansbergen *et al.*, 2004), suggesting a role of CLIP-170 in the dynein–dynactin pathway. During mitosis, an interaction with dynein–dynactin complex targets CLIP-170 to kinetochores (Dujardin *et al.*, 1998; Wieland *et al.*, 2004; Tanenbaum *et al.*, 2006). The C-terminal part of CLIP-170 also binds to the formin homology 2 domain of mDia1; this interaction plays a role in the regulation of actin polymerization during phagocytosis (Lewkowicz *et al.*, 2008).

In our previous study, we demonstrated that the intramolecular interaction between the C and N termini of CLIP-170 inhibits CLIP-170 association with the MT lattice and C-terminal–specific binding partners (Lansbergen *et al.*, 2004). Detailed analysis suggested that the first zinc-knuckle of CLIP-170 and α-tubulin bind to overlapping but not identical sites covering the basic groove of the second CAP-Gly domain of CLIP-170 (Mishima *et al.*, 2007).

CLIP-170 can be phosphorylated on multiple residues in cells and in vitro (Rickard and Kreis, 1991; Choi *et al.*, 2002; Yang *et al.*, 2009). Phosphorylation on Thr[287] by cdc2 positively regulates binding of CLIP-170 to growing MT ends in the G2 phase and the G2/M transition, although it is not essential for CLIP-170 function during other phases of the cell cycle (Yang *et al.*, 2009). Another study indicates that multiple kinases are involved in positive and negative control of CLIP-170 binding to MTs (Choi *et al.*, 2002); however, the biological significance of differential phosphorylation of CLIP-170 is yet to be addressed. We hypothesized that phosphorylation of sites located in the serine-rich regions adjacent to the second CAP-Gly domain regulates the intramolecular interactions of CLIP-170. Using site-directed mutagenesis, we mapped critical sites of phosphorylation in the third serine-rich stretch and demonstrated their significance in regulating CLIP-170 conformational changes, as well as its interaction with MTs and dynactin. Furthermore, by using phosphoproteomic analysis, we determined that S[309] and S[311] of CLIP-170 are phosphorylated in cells and mapped S[311] as a protein kinase A (PKA) phosphorylation site.

MATERIALS AND METHODS

Antibodies

We used mouse monoclonal antibody (mAb) against hemagglutinin (HA; Covance Research Products, Princeton, NJ), green fluorescent protein (GFP; Invitrogen, Carlsbad, CA), α-tubulin (DM1A; Sigma-Aldrich, St. Louis, MO), p150[Glued] and dynamitin (p50) (BD Biosciences, San Jose, CA), rabbit anti-GFP (Invitrogen), and rat anti-α-tubulin mAb (a gift from J. V. Kilmartin; Laboratory of Molecular Biology, Cambridge, United Kingdom). Secondary antibodies were horseradish peroxidase-conjugated donkey anti-mouse and anti-rabbit (Jackson ImmunoResearch Laboratories, West Grove, PA), tetramethylrhodamine B isothiocyanate- and fluorescein isothiocyanate-conjugated donkey anti-mouse and anti-rabbit and Cy5-conjugated anti-rat (Jackson ImmunoResearch Laboratories).

Expression Constructs, Coimmunoprecipitation (coIP), and Western Blotting

HA-tagged expression construct was described by Komarova *et al.* (2002), and GFP-CLIP-170-H1S (4-284) and GFP-CLIP-170-H2 (4-391) were produced by polymerase chain reaction (PCR). Yellow fluorescent protein (YFP)-CLIP-170 was described by Komarova *et al.* (2002). Cyan fluorescent protein (CFP)-YFP tandem and YFP-CLIP-170-CFP were described by Lansbergen *et al.* (2004). All alanine and glutamic acid mutations were introduced by using in vitro site-directed mutagenesis kit (Stratagene, La Jolla, CA). RNA interference (RNAi) expression vector for CLIP-170A was described by Lansbergen *et al.*

(2004). The RNAi cassette was inserted into the AseI site of pECFP-C1. Rescue constructs were prepared by a PCR-based strategy, by introducing triple silent substitutions (underlined) in the target site resulting in a sequence GGAGAAGCA<u>A</u>CA<u>A</u>CACAT<u>C</u>.

For coIP experiments, COS-1 cells were lysed in an immunoprecipitation (IP) buffer (20 mM Tris-HCl, pH 7.5, 100 mM NaCl, 0.5% NP-40, and phosphatase inhibitor cocktail 1 [1:100; Sigma-Aldrich]) as described previously (Komarova *et al.*, 2002). CoIPs and Western blots were performed as described by Hoogenraad *et al.* (2000). For coIP, we used mouse anti-GFP mAb (Roche Applied Science, Indianapolis, IN) and protein G beads (Invitrogen). The bound proteins were dissolved in SDS-polyacrylamide gel electrophoresis (PAGE) sample buffer.

Cell Culture, Transfection, and Treatments

Chinese hamster ovary (CHO)-K1 cells were grown in F-10 medium, and COS-1 and NIH 3T3 cells wee grown in DMEM/F-12 (1:1 mixture) supplemented with 10% fetal bovine serum and antibiotics. Cells were transfected by FuGENE 6 (Applied Science).

Drug treatment was used in some experiments before coIP. COS-1 cells were incubated with 1 μM okadaic acid (OA) or 50 μM staurosporine (Calbiochem, San Diego, CA) for 1 h at 37°C or with 20 μM forskolin (Thermo Fisher Scientific, Waltham, MA) or 200 nM H-89 (Calbiochem) for 30 min at 37°C. Extracts were incubated with calf intestinal phosphatase (20 U; Roche Applied Science) for 1 h at 37°C.

NIH 3T3 and CHO-K1 cells were treated with 10 μg/ml Taxol (Sigma-Aldrich), 20 μM forskolin, and 100 nM or 1 μM OA for 1 h or with 40 μM forskolin, 200 nM H-89, and 10 μg/ml Taxol for 2 h.

Immunostaining, Linescan Analysis, and Quantification of p50 Amount at the MT Tips

Cell fixation, staining, and analysis were performed as described by Komarova *et al.* (2002). In brief, cells were fixed in cold methanol (−20°C), postfixed with 3% formaldehyde, and permeabilized with 0.15% Triton X-100. The samples were imaged by fluorescence deconvolution microscopy using a DeltaVision microscope system (Applied Precision, Issaquah, WA). Images were prepared using Photoshop (Adobe Systems, Mountain View, CA). Linescan analysis, measurements of fluorescence intensity, and densitometry analysis of Western blots were performed using MetaMorph software (Molecular Devices, Sunnyvale, CA). The integrated fluorescence intensities above internal signal were measured within a rectangles covering p50 positively stained tips. Approximately 200 MTs were analyzed in 10–20 control or depleted cells for each experimental condition. Data handling was performed using SigmaPlot software (SPSS, Chicago, IL).

Live Cell Imaging and Quantification of CLIP Kinetics

Analysis of fluorescence decay was performed as described by Komarova *et al.* (2005) and Dragestein *et al.* (2008). Cells were observed at 36°C on a Diaphot 300 inverted microscope (Nikon, Tokyo, Japan) equipped with a Plan 100×, 1.25 numerical aperture objective using YFP filter set. Time-lapse series were acquired with stream acquisition mode. YFP intensity decay was analyzed on 16-bit depth images after subtraction of external background. Curve fitting was applied to determine the decay constant (k_d). Photobleaching was negligible ($k_{bl} = 0.01 \pm 0.004$). Analysis of CLIP-170 fluorescent recovery was performed as described previously (Dragestein *et al.*, 2008), with some modifications (Supplemental Data).

MT-pelleting Assay

Taxol-stabilized MTs were prepared from bovine brain tubulin as described previously (Peloquin *et al.*, 2005). High-speed supernatant extracts were obtained as described by Rickard *et al.*, 1990. An MT-pelleting assay was conducted as described previously (Choi *et al.*, 2002). In brief, COS-1 cells were transfected with YFP-CLIP-170 and its mutants, washed twice with phosphate-buffered saline (PBS), and once with the PEM buffer [0.1 M piperazine-*N*,*N*'-bis(2-ethanesulfonic acid)-KOH, pH 6.8, 2 mM EGTA, 1 mM MgSO$_4$ and 1 mM dithiothreitol; no exogenous ATP was added] at 4°C. The cells were scraped in PEM buffer (2 mM EGTA and 1 mM MgSO$_4$) containing protease inhibitors (Roche Applied Science) at 0°C, Dounce-homogenized, and pelleted by centrifugation sequentially at 40,000 × *g* for 10 min and at 150,000 × *g* for 90 min at 4°C. The high-speed supernatants were incubated with 20 μM Taxol at 37°C for 30 min, and the endogenous MTs were depleted by centrifugation at 30,000 × *g* for 30 min at 20°C. For MT-pelleting assays, 30 μg of total protein of the high-speed supernatant was incubated with Taxol-stabilized MTs in PEM buffer containing 20 μM Taxol at 37°C for 15 min and then centrifuged at 30,000 × *g* for 30 min at 20°C. Resulting pellets were washed in the PEM buffer. Comparable amounts of supernatants and pellets were subjected to SDS-PAGE analysis. YFP-tagged proteins were detected by anti-GFP antibody on Western blot, and tubulin was stained by silver-staining kit (Bio-Rad Laboratories, Hercules, CA).

Measurements of Fluorescence in Cell Extracts

Fluorescence resonance energy transfer (FRET) measurements were performed using a fluorescence spectrometer (PC1 photon counting spectrofluorometer; ISS, Champaign, IL) as described previously (Lansbergen *et al.*, 2004). COS cells were lysed in a buffer consisting of 20 mM Tris-HCl, pH 7.5, 100 mM NaCl, 1% Triton X-100, 10% glycerol, and protease inhibitors (Roche Applied Science). No exogenous ATP was added. Excitation was performed at 425 nm (1 nm bandwidth), and emission spectra were collected in the range 450–600 nm (1 nm bandwidth).

Protein Expression and Purification: In Vitro Phosphorylation and Mass Spectrometry

A tandem fusion construct of rat CLIP-170 head (aa 4-354) with glutathione-S-transferase (GST) at N terminus and 6×His at C terminus were generated in pGEX-4T3 by PCR-based cloning. The proteins were expressed in *Escherichia coli* BL21 and purified by sequential affinity columns on nickel-nitrilotriacetic acid agarose (QIAGEN, Valencia, CA) and glutathione-Sepharose 4B (GE Healthcare, Little Chalfont, Buckinghamshire, United Kingdom) as described by Hegeman *et al.*, 2004. Purified protein (30 μg) was incubated in a manufacturer's reaction buffer and 1 mM ATP with PKA (2500 U; New England Biolabs, Ipswich, MA) for 3–18 h at 30°C. The proteins were denatured by 8 M urea, diluted with 50 mM ammonium bicarbonate, pH 7.5, and digested with 0.6 μg of trypsin for 14 h as described by Hegeman *et al.* (2004).

Tryptic digests were solid phase extracted (using C18 SPEC-PLUS-PT pipette tips; Varian, Lake Forest, CA) and analyzed by microcapillary liquid chromatography-tandem mass spectrometry (MS/MS) using a Micromass Q-TOF2 hybrid quadrupole/orthogonal time of flight mass spectrometer (Waters, Milford, MA). Chromatography of peptides before mass spectral analysis was accomplished using C18 reverse phase high-performance liquid chromatography columns, made in-house, from which eluted species are directly microelectrosprayed. Columns were made using lengths of fused silica tubing (365 μm o.d., 100 μm i.d.) with pulled tips (1-μm orifice) that were packed to 12 cm with Zorbax Eclipse XDB-C18 (Agilent Technologies, Santa Clara, CA), 5-μm, 300Å-pore size media. An Agilent 1100 series HPLC delivered solvents A: 0.1% (vol/vol) formic acid in water, and B: 95% (vol/vol) acetonitrile, 0.1% (vol/vol) formic acid at either 1 μl/min, to load sample, or 150–200 nl/min, to elute peptides over a 180 min 10% (vol/vol) to 70% (vol/vol) B gradient. Voltage was applied upstream of the column through a platinum wire electrode into the fluid path via a PEEK T-junction. As peptides eluted from the HPLC-column/electrospray source, MS/MS spectra were collected from 400 to 2200 *m/z*; redundancy was limited by dynamic exclusion. Collision energy profiles were empirically predetermined for different peptide charge states. MS/MS data were converted to pkl file format by using Micromass Protein Lynx Global Server version 2.1.5 (Waters). Resulting pkl files were used to search a nonredundant (nrNCBI) *Rattus norvegicus* amino acid sequence database by using Mascot Search Engine (Matrix Science, London, United Kingdom), with methionine oxidation; glutamic and aspartic acid deamidation; carbamidomethylation of cysteines and tyrosine; and serine and threonine phosphorylation as variable modifications. Putative modifications identified by Mascot were confirmed using manual assignments of MS/MS spectra.

For analysis of CLIP-170 phosphorylation sites in cells, CLIP-170 was purified by using avidin-biotin affinity-based separation. The tryptic and chymotryptic digests of CLIP-170 were extracted with 50% acetonitrile (MeCN), 5% formic acid (FA) and used for mass spectra analysis (Supplemental Data). The probability of correct phosphorylation site localization was determined for every site in each peptide using the Ascore algorithm (Beausoleil *et al.*, 2006).

RESULTS

Phosphorylation Promotes Intramolecular Association within CLIP-170

The two CAP-Gly domains of CLIP-170 are flanked by three serine-rich stretches. In our previous study, we demonstrated that the N-terminal domain of CLIP-170 (H1; aa 4-309) lacking a part of the third serine-rich stretch binds to the C-terminal domain (Lansbergen *et al.*, 2004). Here, we showed that deletion of the third serine-rich stretch [4-284 mutant, H1S(short); Figure 1 A] increased the binding of N to C termini compared with H2 mutant, which contains all three stretches (4-391; Figure 1B), suggesting that the third serine-rich region might regulate the intramolecular association within CLIP-170. Inhibition of Ser/Thr-specific phosphatases with OA increased the binding of H2 to ΔH but had no effect on the H1S mutant (Figure 1B), indicating that the third serine-rich stretch might contain Ser/Thr residues
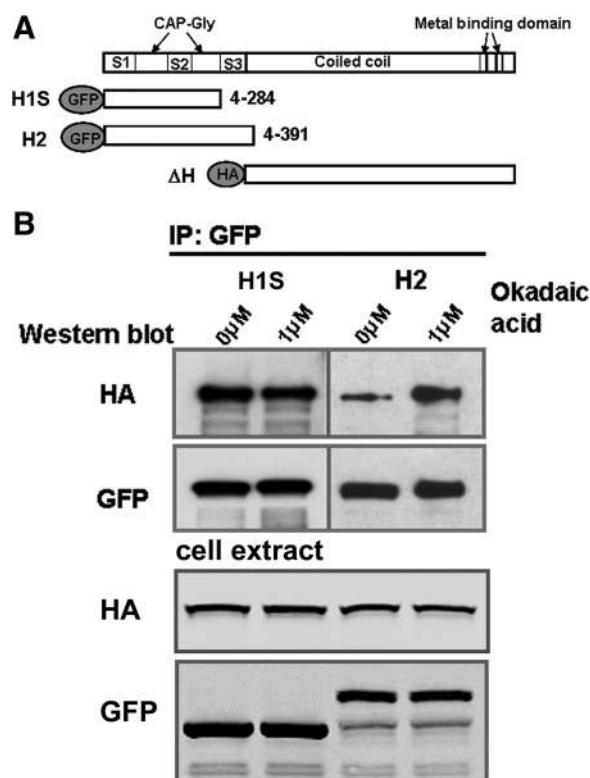

Figure 1. Phosphatase inhibitor OA increases the affinity of H2 domain for C terminus of CLIP-170. (A) Schematic representation of CLIP-170 deletion mutants. S, serine-rich stretches; H, head domain. (B) The interaction between H1S or H2 and C-terminal domains. COS-1 cells coexpressing CLIP-170 deletion mutants (indicated in A) were left untreated or pretreated with OA for 30 min and were used for coIP with anti-GFP mAb. Resulting precipitates were probed with HA mAb and GFP polyclonal antibody. The relative expression levels of exogenous proteins is shown below, 3% of the whole cell extracts used for coIP. Note that deletion of the third serine-rich stretch increased the affinity of the head domain for the C terminus. Inhibition of phosphatases with OA altered the binding of H2 to ΔH but had no effect on the H1S mutant.

phosphorylation of which induces intramolecular interactions within CLIP-170.

Mapping of Potential Regulatory Sites

We sought to determine the critical residues involved in regulation of CLIP-170 intramolecular association. The third serine-rich stretch of CLIP-170 contains 17 serine residues, 16 of which are highly conserved among mammals (Figure 2A). By using site-directed mutagenesis, we generated phosphorylation-deficient (Ser→Ala) and phosphomimetic (Ser→Glu) mutants of YFP-CLIP-170 and assessed their binding to MT tips and to Taxol-stabilized MTs in cells (Table 1). Because intramolecular association within CLIP-170 significantly reduces its affinity for MTs (Lansbergen *et al.*, 2004), we reasoned that mutants predominantly possessing an "open" conformation may display increased MT affinity. In line with this idea, a mutation in the first zinc-knuckle (Goodson *et al.*, 2003; Lansbergen *et al.*, 2004) that alters the intramolecular associations, induced binding of protein to MTs in Taxol-treated cells (unpublished data). The distribution of YFP-CLIP-170 mutants was assessed by live cell imaging (Supplemental Figure 1) and by immunofluorescence (Figure 2B). Because overexpression alters
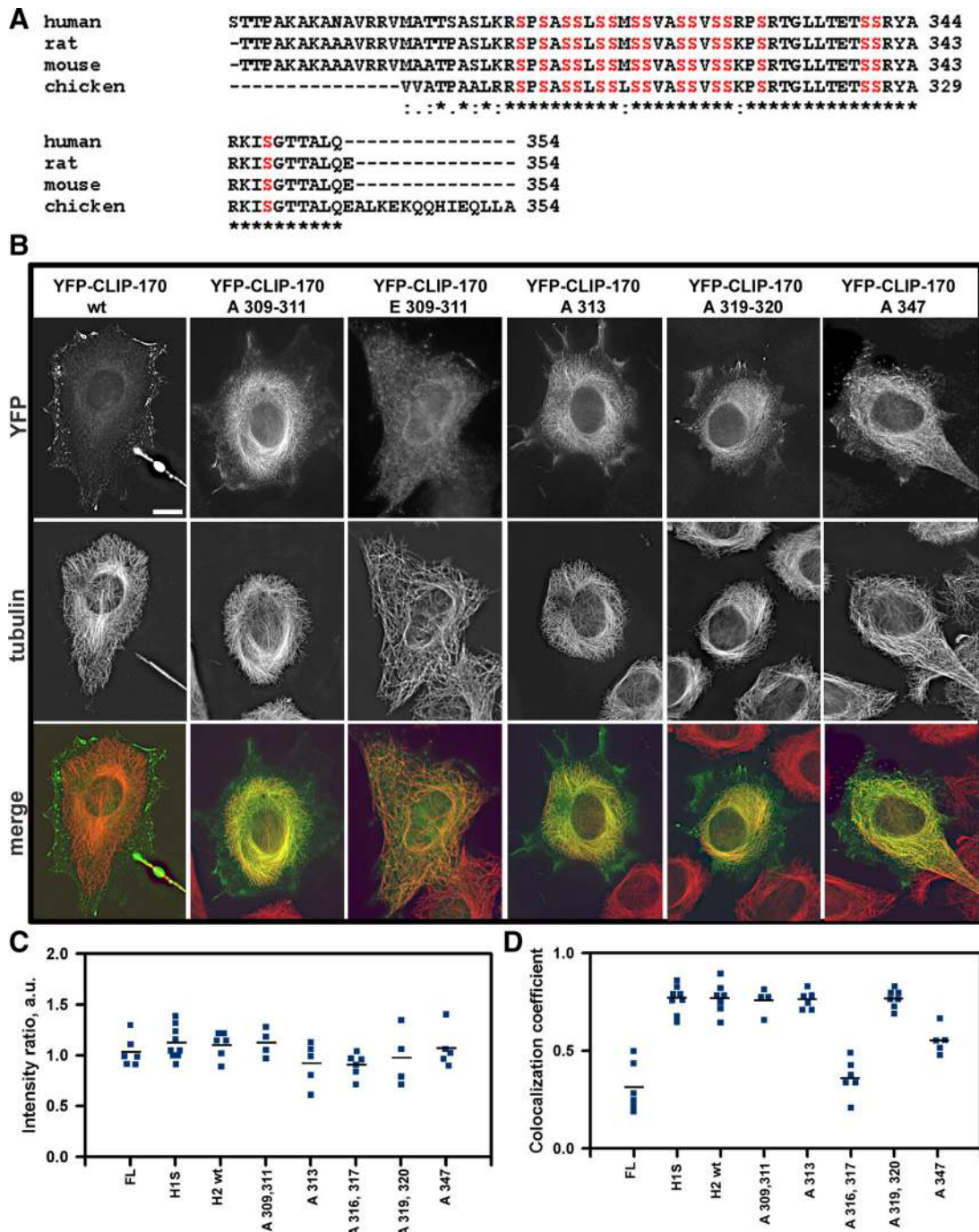
Figure 2. Mapping of critical residues located in the third serine-rich region of CLIP-170. (A) Sequence alignment of the third serine-rich region of CLIP-170 for human, rat, mouse and chicken. Conserved serine residues are highlighted in red. * - residues identical in all sequences in the alignment; : - conservative substitutions; . - semiconservative substitutions. (B) Representative images of 3T3 NIH fibroblasts expressing either YFP-CLIP-170 or its mutants. Images were collected using the same setting for each channel between experiments. YFP-CLIP-170 does not bind stabilized MTs in Taxol-treated cells. Mutation of serines 309, 311, 313, 319, 320, and 347 to alanines resulted in binding of mutants to Taxol MTs. Mutation of the same residues to glutamic acid (except for $S^{347}E$) did not cause binding to stabilized MTs (shown for YFP-CLIP-170-E$^{309, 311}$). In the overlay GFP is green and tubulin is red. Bar, 10 μm. (C) Relative expression levels of different CLIP-170 mutants presented as a ratio of integrated intensity of GFP/tubulin in the whole cell. Each data point represents a cell. Cells exhibiting ratios within the range of 0.5–1.5 were selected for further analysis. (D) Colocalization of CLIP-170 mutants with stabilized MTs was analyzed using the same set of cells as represented in C. Colocalization coefficients were calculated from the scatter plots for GFP and tubulin using LSM software and Z-stack images (Carl Zeiss MicroImaging Inc, Jena, Germany). Each data point represents a cell. The black lines in C and D indicate the average values.

CLIP-170 behavior in cells, thus resulting in the longer labeled stretches at the MT ends (Goodson *et al.*, 2003), we selected only the cells expressing relatively low levels of

exogenous proteins. In particular, we determined the relationship between the length of CLIP-170–positive comets and the average intensities of YFP signals at the MT ends by

Table 1. Binding of CLIP-170 mutants to MT tips and lattice

Mutated site(s)	Binding to MTs in Taxol-treated cells[a]		Length of MT tips, live imaging, μm
	Live imaging	Staining	
1. Wild type	−	−	1.26 ± 0.28
in the third serine-rich domain			
2. Ser309-311A	++	++	1.8 ± 0.4; p < 0.0001[b]
Ser309-311E	−	−	1.0 ± 0.19; p < 0.0001
3. Ser313A	++	++	1.36 ± 0.26; p < 0.001
Ser313 E	+	+	1.2 ± 0.20
4. Ser314A	−	−	1.2 ± 0.26
5. Ser316-317A	N.A.[c]	−	1.22 ± 0.3
6. Ser319-320A	++	++	1.4 ± 0.36; p < 0.0001
Ser319E	N.A.	−	1.0 ± 0.24; p < 0.0001
7. Ser323-324A	−	−	1.4 ± 0.43; p < 0.001
8. Ser326-327A	−	−	1.2 ± 0.26
9. Ser330A	−	−	1.2 ± 0.2
10. Ser339-340A	−	−	1.22 ± 0.3
11. Ser347A	+	+	1.21 ± 0.24
Ser347E	+	+	1.10 ± 0.12
12. Ser309-311-326-327A	++	N.A.	1.84 ± 0.5; p < 0.0001
13. Ser309-347A	+	N.A.	N.A.
14. Ser309-311-320A	++	N.A.	1.85 ± 0.46; p < 0.0001
15. Ser309-311-313-319-320A	++	++	3.04 ± 0.6; p < 0.0001
16. Ser309-311-313-319-320 E	−	−	0.7 ± 0.15; p < 0.0001
in the second serine-rich region			
17. S146A	+	N.A.	1.34 ± 0.28
18. S149-192A	−	N.A.	1.14 ± 0.2
19. T188A	−	N.A.	1.0 ± 0.19; p < 0.0001
20. S194A	+	N.A.	1.2 ± 0.18
21. S203A	+	N.A.	1.2 ± 0.24

[a] ++, strong binding; +, moderate binding; −, no binding.
[b] p values were obtained based on *t* test compared with the length of nonmutated CLIP-170.
[c] N.A., not applicable.

using the wild-type (wt) protein (Supplemental Figure 1) for which we previously estimated the average length in the CHO-K1 stable cell line (Komarova *et al.*, 2005). Based on this analysis, we then selected the cells expressing different CLIP-170 mutants showing the average intensities of YFP signals within the same range as for the wt protein (Supplemental Figure 1). For immunofluorescence staining, the expression levels were controlled by the YFP/tubulin integrated intensity ratio (Figure 2C). The colocalization of YFP-CLIP-170 mutants with MTs in Taxol-treated cells was determined by immunofluorescent staining and expressed by colocalization coefficient (Figure 2D). The S^{309}A, S^{311}A, S^{313}A, S^{319}A, and S^{320}A mutants displayed both a statistically significant increase in the length of YFP-CLIP-170–positive stretches at the MT tips (Table 1 and Supplemental Figure 1) and the binding along the MTs in Taxol-treated cells (Figure 2B). Mutation of the same residues for glutamic acid led to shorter YFP-CLIP-170 structures at MT tips (Table 1). Similar to wild-type CLIP-170, phospho-mimetic mutants displayed no MT binding in Taxol-treated cells (Figure 2B; shown for S$^{309−311}$E). The mutation of S^{347} to either Ala or Glu had no effect on CLIP-170 distribution at MT tips; however, both mutations induced moderate binding of CLIP-170 to Taxol-stabilized MTs in cells, suggesting that phosphorylation of this residue might not be directly involved in modulation of MT affinity (Table 1 and Figure 2, B–D).

Phosphomimicking Mutations Promote Folding of CLIP-170

Next, we determined whether mutation of the six identified residues regulates affinity of N to C termini. HA-CLIP-170-ΔH was coexpressed with either phosphomimetic or phosphorylation-deficient CLIP-170-H2 mutants; coexpression with H1 or nonmutated H2 was used as controls. Individual mutations of S^{309}, S^{311}, S^{319}, and S^{320} to glutamic acid markedly increased the amount of coimmunoprecipitated ΔH, whereas mutation of S^{313} had a marginal effect (Figure 3A). Consistent with this observation, mutation of the same residues to alanine greatly diminished the amount of coimmunoprecipitated ΔH, except for S^{309} and S^{313}, which were similar to nonmutated H2 (Figure 3A). However, mutation of both S^{309} and S^{311} to alanine decreased the amount of immunoprecipitated ΔH significantly more than S^{309} or S^{311} alone, suggesting that dephosphorylation of S^{309} and S^{311} might have an additive effect on establishing an open CLIP-170 conformation. Mutation of S^{311} led to the most significant increase in association of N and C termini, suggesting that phosphorylation of S^{311} may be critical for establishing the "folded back" conformation of CLIP-170. Furthermore, mutation of all five serine residues to alanine (designated as A-5 mutant) abolished the interaction between N and C termini, whereas substitution of the same residues for glutamic acid greatly increased the amount of coimmunoprecipitated ΔH (Figure 3A). Overall, coimmunoprecipita-
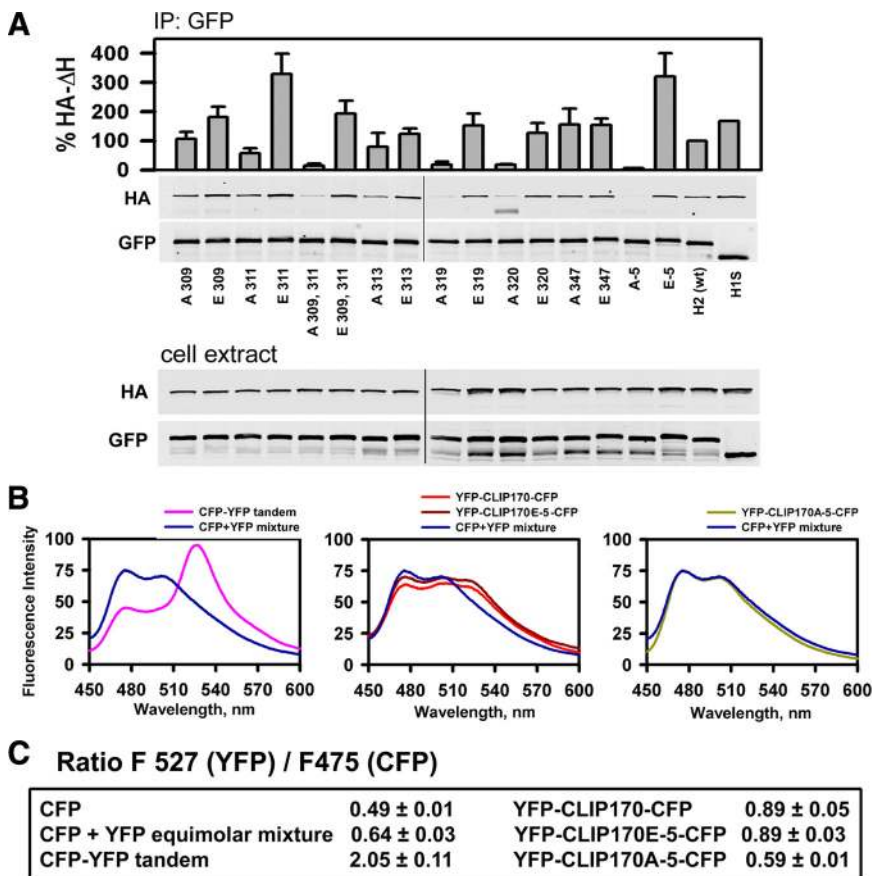
Figure 3. Identification of serine residues affecting intramolecular association and conformational changes in CLIP-170. (A) CoIP of HA-ΔH with GFP-H2 mutants. Lysates were prepared from COS-1 cells transiently coexpressing the indicated GFP-H2 mutants together with ΔH; immunoprecipitation was performed with anti-GFP mAb. Western blots were probed with anti-HA to detect bound ΔH and with anti-GFP antibodies to detect the H2 mutants. The relative expression level of exogenous proteins is shown below, 3% of the whole cell extracts of the "input" samples used for coIP. The bar plot represents the relative amounts of coimmunoprecipitated ΔH (normalized to IP GFP-H2). The amount of ΔH coIP with H1S mutant was assigned as 100%. Mean ± SD was determined from three independent experiments. (B) FRET analysis of YFP-CLIP-170-CFP fusion and its mutants. Five serine residues at positions 309, 311, 313, 319, and 320 were substituted either with alanine (A-5) or with glutamic acid (E-5). Uncorrected emission spectra of cell extracts measured with the excitation at 425 nm. Fluorescence intensity is shown in arbitrary units. FRET signal of the equimolar mixture of YFP and CFP (negative control) is shown in each graph for comparison. (C) Ratios of emission at 527 nm (YFP acceptor) to 475 nm (CFP donor). Mean ± SD was determined from three independent measurements.

tion assay results were consistent with binding of these mutants to MT tips and Taxol-stabilized MTs.

To confirm that phosphorylation of identified residues regulates the conformation of CLIP-170, we performed FRET analysis on extracts of cells expressing a YFP-CLIP-170-CFP fusion (Lansbergen *et al.*, 2004) in which all five serine residues were replaced with either alanine or glutamic acid. As a negative control, we used a mixture of extracts prepared from cells expressing either CFP or YFP; CFP-YFP tandem fusion was as a positive control. A mixture of cell extracts containing equimolar CFP and YFP proteins displayed no significant emission of the YFP acceptor after excitation of the CFP donor, giving a fluorescence ratio at 527/475 nm similar to that obtained for CFP alone (Figure 3, B and C). In contrast, the CFP-YFP tandem displayed a prominent peak of YFP emission (Figure 3B). A smaller but significant YFP-sensitized emission peak was detected for nonmutated YFP-CLIP-170-CFP and its E-5 mutant (Figure 3B). FRET expressed as the ratio of fluorescence obtained at 527 and 475 nm for wild-type CLIP-170 was consistent with published data (Lansbergen *et al.*, 2004) and was indistinguishable from FRET observed for the E-5 mutant (Figure 3C). This means that a significant proportion of wild-type CLIP-170 might possess a folded back conformation in cells; alternatively, our FRET assay might be insensitive to the increase of CLIP-170 self-folding beyond a certain point due to its potentially transient character (Lansbergen *et al.*, 2004). The YFP-CLIP-170-A-5-CFP mutant produced no significant emission from the acceptor after excitation of the donor; its FRET signal was similar to the negative control (Figure 3D), indicating that phosphodeficient CLIP-170 possesses an

open conformation. FRET results suggest that the phosphorylation state of the identified serine residues may determine conformational changes of CLIP-170.

Phosphorylation-deficient Mutant Demonstrates Increased Affinity to Growing MT Ends

We proposed previously that conformational changes of CLIP-170 control its interaction with the MT lattice (Lansbergen *et al.*, 2004). Using an MT copelleting assay, we observed a dramatic difference in the binding affinities of phosphomimetic and phosphorylation-deficient CLIP-170 to the MT lattice. The CLIP-170A-5 mutant was completely sedimented with Taxol-stabilized MTs at a tubulin concentration of 0.5 μM (Figure 4, A and B), whereas <30% of the CLIP-170E-5 mutant was sedimented at 20 μM tubulin (Figure 4, A and B; unpublished data).

Next, we used live imaging to assess kinetics of CLIP-170A-5 and E-5 mutants at the growing MT ends. WT and both mutants bound to the MT growing ends, suggesting that dephosphorylation of these five residues is not required for MT tracking (Figure 4, C–D, and Table 1). The analysis of the relationship between intensities and the lengths of CLIP-170 structures suggested that phosphorylation might regulate affinity of CLIP-170 to growing MT ends (Figure 4E; n = 300 MTs for each group). The phosphorylation-deficient CLIP-170 mutant associated with longer MT segments (3.04 ± 0.6 μm; p < 0.0001), whereas the phosphomimetic mutant labeled only outer most MT segments (0.7 ± 0.15 μm; p < 0.0001).

The distinct length distribution of mutants predicted the difference in fluorescence decay at MT ends. Consistent with
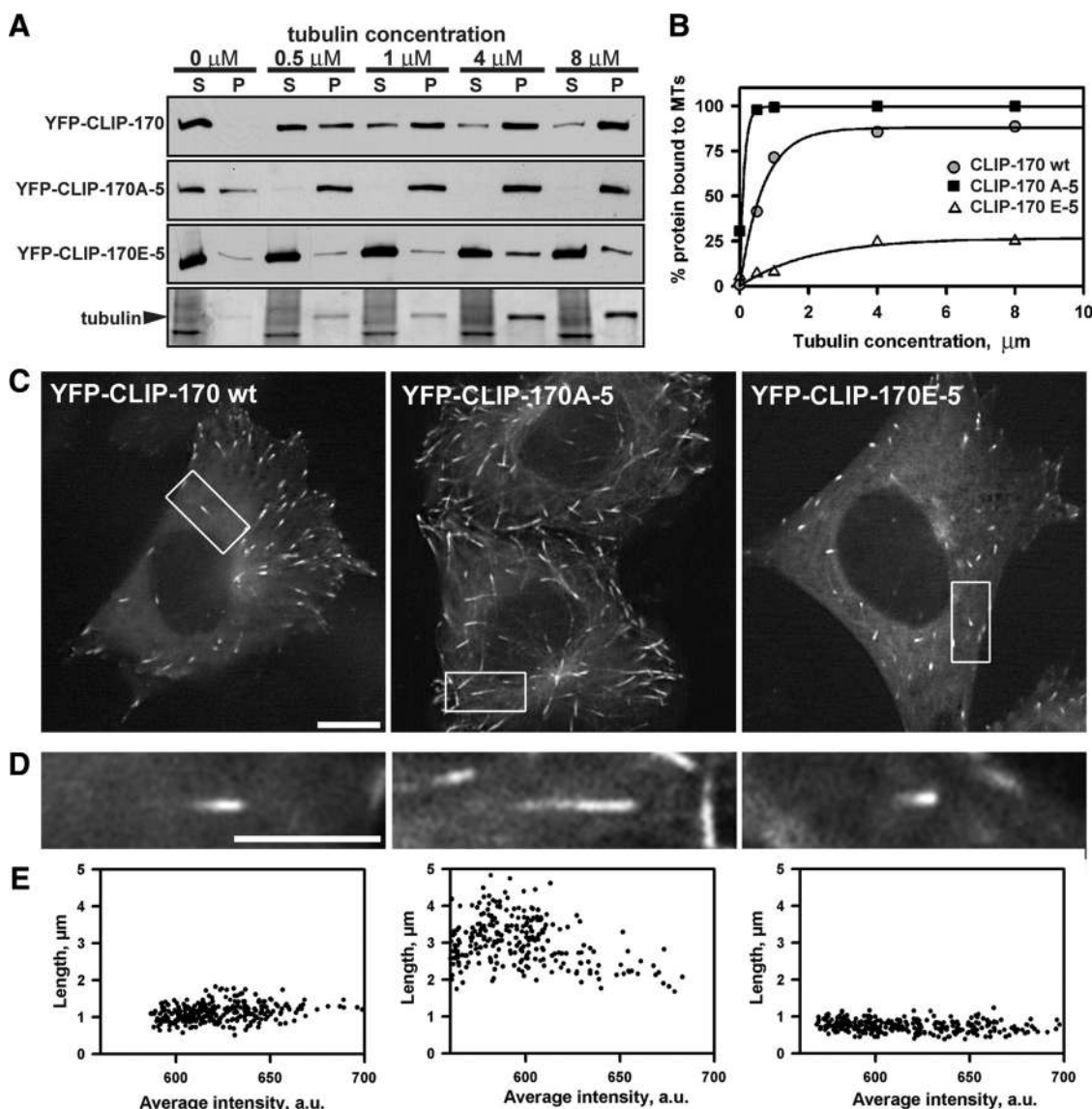
Figure 4. Effects of CLIP-170 mutations on binding to MT lattice and MT tips. (A) MT pelleting assays with YFP-CLIP-170, A-5, and E-5 mutants. The assays were performed with cell extracts prepared from COS-1 cells expressing YFP-CLIP-170 or its mutants. Concentrations of added Taxol MTs varied from 0 to 8 μM as indicated. Western blots were probed with anti-GFP mAb; tubulin was detected by silver staining. S, supernatant; P, pellet. (B) The amount of protein bound to Taxol MTs was estimated based on densitometry analysis of immunoblots (sum of protein in supernatant and pellet was taken for 100%) and plotted versus the concentration of added Taxol MTs. The best fit to the data demonstrated the difference in affinity of A-5 and E-5 to Taxol MTs. (C–G) Binding of YFP-CLIP-170 and its mutants to the MT tips. (C) Representative live images of CHO-K1 cells expressing YFP-CLIP-170, A-5, and E-5 mutants. (D) Enlarged images from the rectangular boxes in C. Bar, 5 μm. (E) Distribution of CLIP-170 and mutants at the MT tips. The length of YFP-positive structures was plotted versus the average intensity of YFP signal at the MT ends. Each data point represents an individual MT end; n = 300 MTs in 30 cells (~10 MTs/cell) were analyzed for each mutation. (F) The plots show fluorescent intensity decay at the MT tips over time (average of 40 MTs ± SE). The images were collected using the stream mode of MetaMorph software and 100-ms exposure time. Images were utilized for kymograph analysis after background subtraction. The intensity decay at the distal MT ends was measured within 1 pixel using linescan analysis. The digital data were used to recalculate each data point and to normalize maximum value to 60 arbitrary units (a.u.). The data originated from analysis of 40 MT ends were averaged and plotted as a scatter plot with the error bar. Each data point represents the fluorescence intensity at the MT end over time for 40 MTs. The exponential curve fitting was used to determine the decay constant, k_d (line plot on the graph). (G) Fast FRAP analysis of YFP-CLIP-170 and A-5 mutant in COS cells. Fluorescence intensity over time was measured along the lines of a 3-pixel width (200 nm) and a 250-pixel length (~7.5 s), starting 25 pixels (i.e., ~750 ms) before the bleaching. Mean fluorescence decay in nonbleached areas (blue; 14 measurements for YFP-CLIP-170 and 12 for A-5) and recovery in bleach areas (red; 18 FRAP curves for YFP-CLIP-170 and 31 for A-5) after photobleaching. Mean fluorescence recovery on MT ends (*k*) is indicated. Details of FRAP analysis are provided in Supplemental Figure 3.

published results (Folker *et al.*, 2005; Komarova *et al.*, 2005; Dragestein *et al.*, 2008), the decrease of YFP-CLIP-170 fluorescence at MT tips could be fitted to an exponential decay curve. The fluorescent decay constant (k_d) for wild type was

0.45 ± 0.13 s^{-1} corresponding to an apparent half-life of 1.6 ± 0.5 s (n = 30) for the CLIP-170 binding sites (Figure 4F). The phosphorylation-deficient mutant displayed a considerably reduced decay constant of 0.24 ± 0.09 s^{-1} (half-life
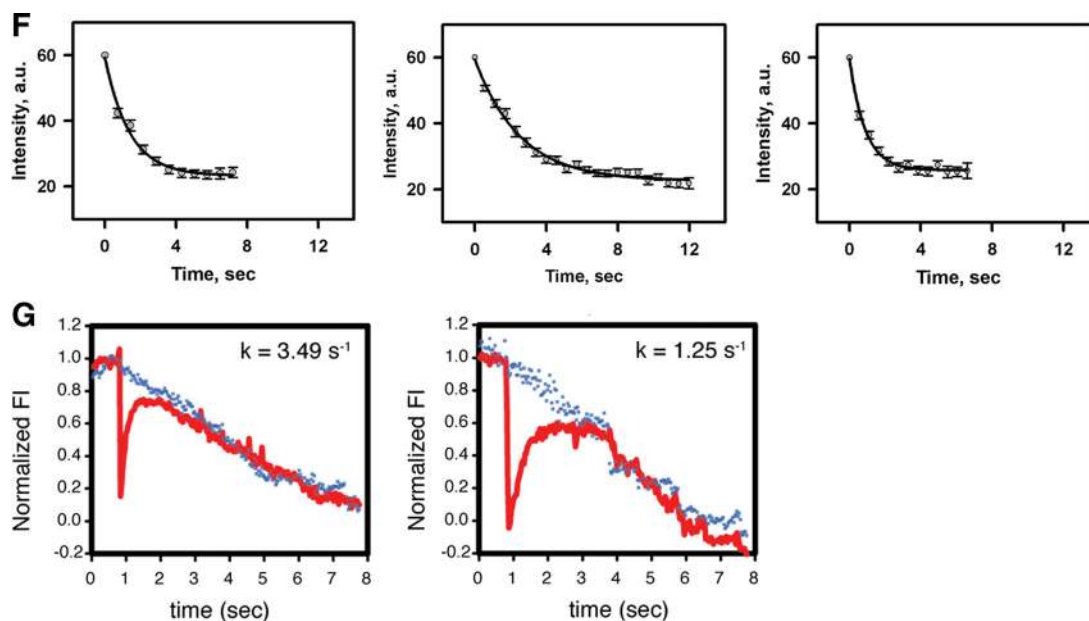
Figure 4. *Continued.*

3.23 ± 1.19 s; n = 37; Figure 4F), whereas the phosphomimic mutant had an increased decay constant of 1.05 ± 0.43 s^{-1} (half-life 0.76 ± 0.29 s; n = 40; Figure 4F). The expression of CLIP-170 mutants had no effect on the rate of MT growth. The instantaneous growth rates were 23.2 ± 4.9, 25.7 ± 5.1, and 24.6 ± 7.2 μm/min for wild-type, phosphomimetic, and phosphodeficient mutants, respectively (n = 60 MTs for each experimental condition), demonstrating that the distinct length distribution of CLIP-170 mutants was not due to the changes in MT growth rates. Therefore, we address whether CLIP-170 mutants might have a distinct affinity to the growing MT ends. The kinetics of CLIP-170 was determined previously by a fast fluorescence recovery after photobleaching (FRAP; Dragestein *et al.*, 2008). Here, we used an improved protocol using total internal reflection fluorescence (TIRF) microscopy. The YFP-positive structures were detected by real-time TIRF imaging, and tips of the comets were bleached within circular spots. An apparent $k_{recovery}$ was 3.49 s^{-1} for wild-type YFP-CLIP-170 (Figure 4G and Supplemental Figure 3), which is close to the value obtained previously for GFP-CLIP-170 (Dragestein *et al.*, 2008). Interestingly, the phosphodeficient mutant of CLIP-170 displayed a $k_{recovery}$ of 1.25 s^{-1} (Figure 4G), suggesting that it exchanges slower than wild-type CLIP-170. These data indicate that CLIP-170 is largely phosphorylated in cells and are in agreement with FRET analysis.

Gain of CLIP-170 Function Interferes with Dynein-mediated Trafficking

Previously, we proposed a regulatory role for CLIP-170 conformational changes in recruitment and release of the dynactin complex at MT plus ends (Lansbergen *et al.*, 2004). Here, we tested whether CLIP-170 mutants display a difference in recruitment of dynactin to MT tips. We replaced endogenous CLIP-170 either with A-5 or with E-5 mutants and evaluated the distribution and amount of endogenous p50, a subunit of the dynactin complex, at MT tips. Expression of YFP-CLIP-170 was used as a control. The endogenous CLIP-170 was depleted with plasmid-based RNAi (Brummelkamp *et al.*, 2002). The RNAi cassettes containing a

previously described target region (Lansbergen *et al.*, 2004) were inserted into pECFP-C1 vector for detection of transfected cells; YFP-CLIP-170 or its mutants in which we introduced three silent substitutions in the siRNA target region were used for rescue experiments. Cells expressing both the CFP reporter and YFP-tagged proteins were analyzed.

In nontransfected CHO-K1 cells, p50 displayed "dot"-like structures, with an average length of ~1 μm at MT tips (Figure 5, A and D, enlarged 1). Expression of YFP-CLIP-170 slightly increased p50 accumulation at the MT distal ends (Figure 5A, enlarged 2), resulting in ~1.5-μm-long segments (Figure 5E). Expression of the YFP-CLIP-170 A-5 mutant led to even longer ~4-μm segments of p50 (Figure 5, B and F, enlarged 2). The YFP-CLIP-170 E-5 mutant had the opposite effect (Figure 5C, enlarged 2), reducing both the length of p50 structures and the peak intensity (Figure 5G). To evaluate the relative amount of dynactin bound to the MT tips, we quantified the integrated fluorescence intensity of the p50 signal within rectangles circumscribing the entire positively stained tip (Figure 5H). We found that accumulation of p50 compared with surrounding nontransfected cells was slightly enhanced to 127 ± 36% by expression of YFP-CLIP-170 and slightly reduced to 74 ± 30% by expression of the phosphomimetic mutant. The most dramatic change was observed after expression of the phosphorylation-deficient mutant that increased the recruitment of p50 by nearly threefold (258 ± 67%). These data support the view that targeting of dynactin to MT tips might depend on CLIP-170 phosphorylation state.

CLIP-170 interacts directly with p150[Glued], the large subunit of dynactin complex, and this interaction occurs via the second zinc knuckle of CLIP-170 and the CAP-Gly motif of p150[Glued] (Goodson *et al.*, 2003; Lansbergen *et al.*, 2004; Weisbrich *et al.*, 2007). YFP-CLIP-170 and the phosphomimetic mutant weakly interacted with endogenous p150[Glued], whereas the A-5 mutant strongly bound to p150[Glued] as demonstrated by coimmunoprecipitation study (Figure 5I). We conclude that phosphorylation might regulate CLIP-170 affinity for dynactin either directly or indirectly via modulation of CLIP-170 conformation.
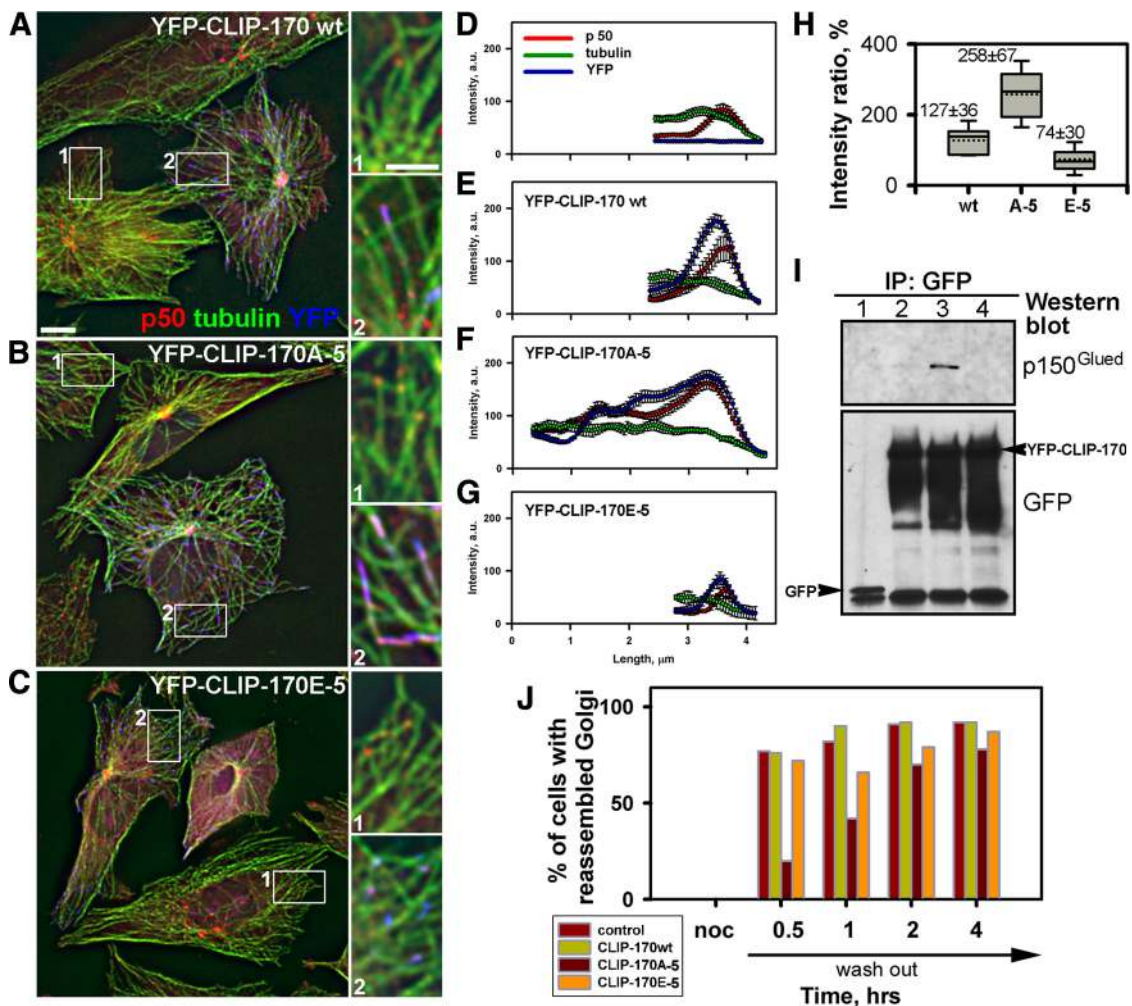
Figure 5. Dephosphorylation site mutations increases affinity of CLIP-170 for dynactin and delays Golgi reassembly. (A–C) The distribution of dynactin at MT tips in cells depleted of CLIP-170 and re-expressing CLIP-170 mutants. CHO-K1 cells expressing CFP-tagged shRNA to CLIP-170 and either YFP-CLIP-170 (A) and A-5 (B) or E-5 (C) mutants (blue in overlay) were stained for p50 (red) and tubulin (green). Enlarged images of control (1) or expressing (2) cells are shown from the right. Bar, 5 μm. (D–G) Fluorescence intensity profiles for p50 (red); YFP (blue) and tubulin (green) at the distal MT ends in nontransfected cells (D); cells expressing YFP-CLIP-170 (E), A-5 (F), or E-5 (G) mutants. The average intensity of 20 MTs ± SE. (H) The accumulation of p50 at the MT tips relative to expression of CLIP-170 or mutants. The integrated intensity of p50 was expressed as a percentage of the intensity in control cells from the same image, which was taken for 100% and plotted as box graphs. The boundaries of the box and whiskers indicate the 25th and the 75th percentile, and the 90th and 10th percentiles, respectively. The median and mean are shown by a straight and a dotted line, respectively. The numbers on the graphs indicate the average values and standard deviations. The values are statistically different with 95% confidence of nonoverlapping intervals. (I) Dephosphorylation site mutations increase affinity of CLIP-170 for p150[Glued]. Lysates prepared from COS-1 cells expressing GFP (1), YFP-CLIP-170 (2), A-5 (3), or E-5 (4) were used for IPs with anti-GFP antibodies. Resulting precipitates were probed with antibodies against GFP and p150[Glued]. Arrowheads indicate GFP and YFP-CLIP-170 bands; additionally detected bands result from cross-reaction with immunoglobulin G heavy chain. (J) Time course of Golgi reassembly after nocodazole-induced scattering. CHO-K1 cells coexpressing CFP-GalT and YFP-CLIP-170 mutants were used to score percentages of cells with reassembled Golgi at the different times after nocodazole washout. Cells expressing only CFP-GalT were used as a control. Cells expressing YFP-CLIP-170A-5 display significant delay in Golgi reassembly.

Next, we tested whether CLIP-170 phosphorylation contributes to dynein-dependent transport of membrane organelles. We found no mislocalization of the Golgi apparatus in cells transiently coexpressing CFP-tagged β-1,4-galactocyltransferase (CFP-GalT) and YFP-tagged mutants in steady state (Supplemental Figure 2). However, expression of CLIP-170 phosphorylation-deficient mutant caused a significant delay in Golgi reassembly (up to 4 h) after nocodazole-induced scattering (Figure 5J and Supplemental Figure 2), whereas the majority of control cells or cells expressing YFP-CLIP-170 or E-5 mutant showed Golgi recovery within 30 min. Our results dem-

onstrate that CLIP-170 dephosphorylation induces increased binding to dynactin and interferes with minus-end–directed membrane trafficking, and we suggest that CLIP-170 phosphorylation status might be important for efficient dynein function.

Phosphoproteomic Analysis of CLIP-170 Phosphorylation Sites in Cell

We used phosphoproteomic analysis to determine phosphorylation sites of CLIP-170 in cells. CLIP-170 was phosphorylated on multiple serine and threonine residues in cells pretreated with the phosphatase inhibitor calyculin

A (Supplemental Figure 4). We confirmed phosphorylation of S^{309}, S^{311}, S^{314}, and S^{347} in cells. The effect of these sites on CLIP-170 function was described above. In addition, we found several phosphorylation sites in the second serine-rich stretch, which are also adjacent to the second CAP-Gly domain (Supplemental Figure 4). To determine whether phosphorylation of these residues might regulate binding of CLIP-170 to MTs, we substituted S^{146}, S^{149}, T^{188}, S^{192}, S^{194}, and S^{203} with alanine and determined the length distribution of these mutants at the MT tips in 3T3

fibroblasts (Table 1). We found that the S^{146}A mutant displayed a significant increase in the comet length at the MT ends and could bind to Taxol-stabilized MTs in cells. This finding is in an agreement with coimmunoprecipitation data (Supplemental Figure 5), suggesting that mutation of S^{146} for Ala reduces the affinity between the N and C termini. In contrast to S^{146}, mutation of Thr^{188} for A resulted in reduced binding to MT tips. Moderate binding to MTs in Taxol-treated cells also was observed for S^{194}A and S^{203}A, whereas the other mutations had no effect.
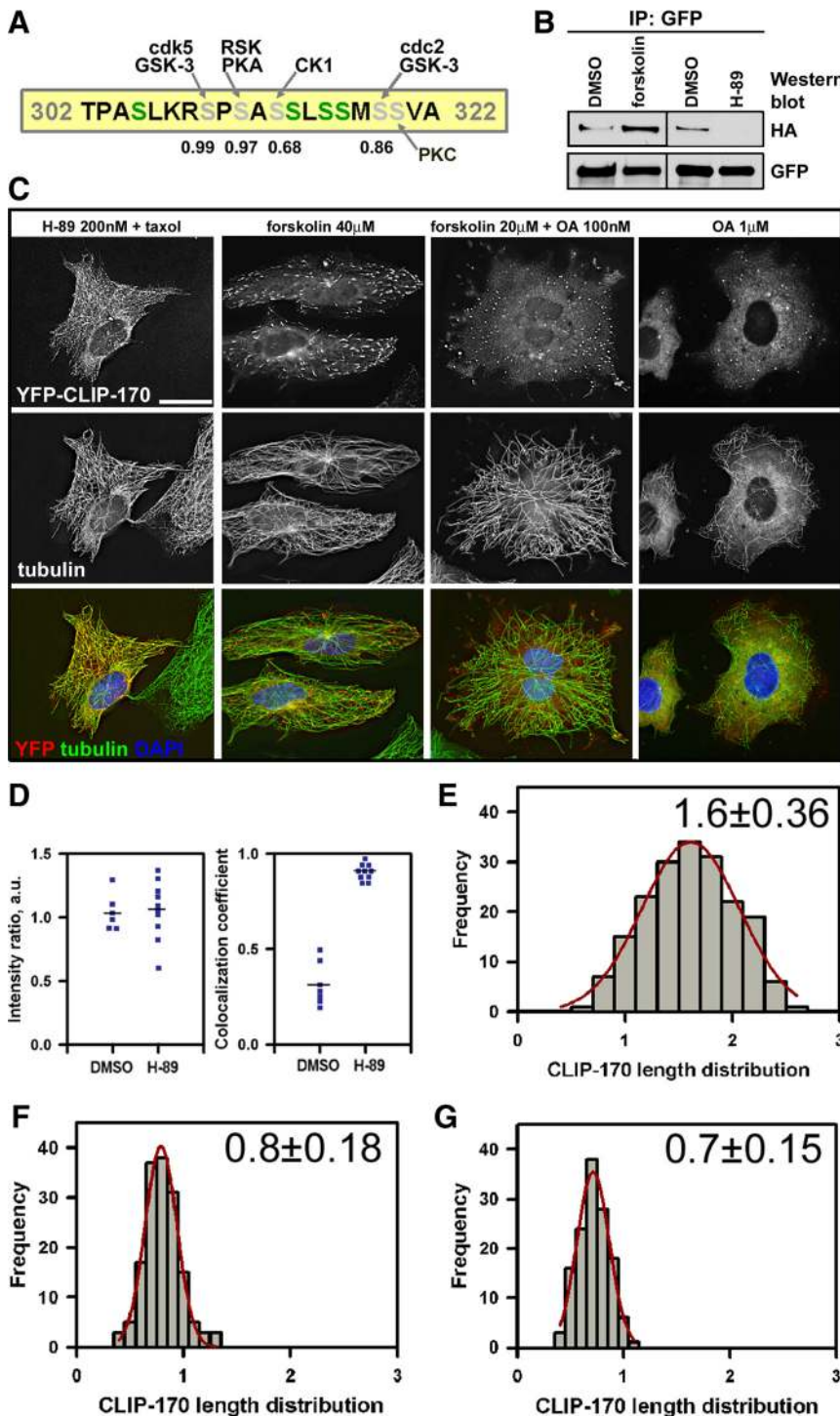

Figure 6. PKA regulates CLIP-170 intramolecular interaction and binding to MTs. (A) Predicted kinase-specific phosphorylation sites in the third serine region of CLIP-170. Amino acids 302-322 from rat CLIP-170 are shown. S^{309} is a predicted Glycogen synthase kinase (GSK)-3 and cdk5 site, S^{311} is a RSK and PKA site, S^{313} is CK1 site, S^{319} is GSK-3 and cdc2 site, and S^{320} is PKC site. Critical serine residues are in gray; noncritical residues are in green; numbers indicate phosphorylation scores. (B) Effect of PKA activation (forskolin) and inhibition (H-89) on CLIP-170 intramolecular interaction. COS-1 cells coexpressing GFP-H2 and HA-ΔH domains of CLIP-170 were treated with dimethyl sulfoxide (DMSO), 40 μM forskolin, or 0.2 μM H-89. Cell lysates were used for IPs with anti-GFP antibodies, and resulting precipitates were probed with antibodies against HA and GFP. Activation of PKA increases the amount of coprecipitated ΔH domain, whereas inhibition abolishes this interaction. (C) PKA modulates CLIP-170 binding to MTs in cells. CHO-K1 cells expressing YFP-CLIP-170 were treated with 200 nM H-89 and 10 mg/ml Taxol for 2 h; 40 μM forskolin or 20 μM forskolin and 100 nM okadaic acid (forskolin + OA) or 1 μM okadaic acid (OA) for 1 h. Cells were fixed and stained for YFP (red in overlay), tubulin (green), and DNA (4,6-diamidino-2-phenylindole [DAPI]; blue). Bar, 10 μm. (D) The binding of YFP-CLIP-170 to Taxol-stabilized MTs in cells pretreated with DMSO and H-89. Relative intensity and colocalization coefficient were quantified as described in Figure 2. Inhibition of PKA led to the binding of CLIP-170 to MTs in Taxol-treated cells. (E–G) Histograms of distributions of the YFP–CLIP-170–positive MT tip lengths in cells treated with forskolin (E), forskolin + OA (F), and OA (G). Mean ± SD is indicated in the corner of each graph. n = 150 MTs for each condition.
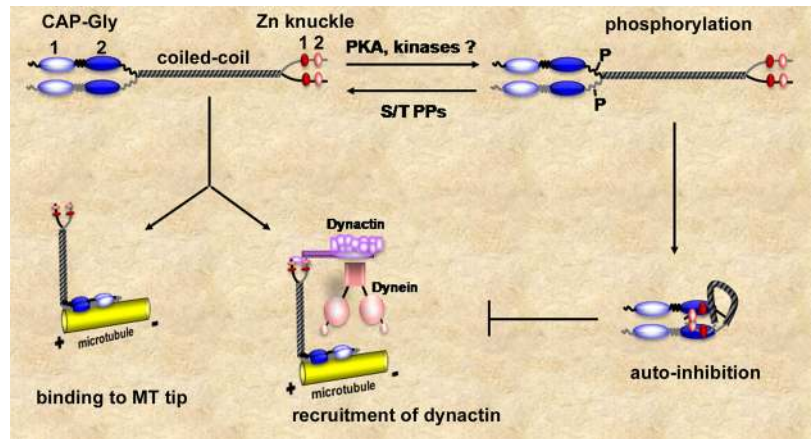
Figure 7. Model of phosphorylation-mediated autoinhibition of CLIP-170. CLIP-170 consists of two CAP-Gly domains surrounded by three serine-rich regions at N terminus; coiled-coil and two zinc-knuckles at the C terminus. Dephosphorylated CLIP-170 possesses open conformation and binds to MT tips and dynactin with high affinity. Phosphorylation of CLIP-170 on serine residues located in the third serine-rich region induces CLIP-170 conformational changes resulting in CLIP-170 autoinhibition. CLIP-170 possessing folded conformation exhibits low affinity to MT tips and dynactin.

These data suggest that S^{146} and T^{188} also might be involved in regulating CLIP-170 binding to MTs.

PKA Phosphorylates CLIP-170 at S^{311}

We aimed to determine the kinase responsible for phosphorylation of S^{311} because mutation of this residue had the most profound effect on CLIP-170 intramolecular association. A database search (Scansite [http://scansite.mit.edu/] and NetPhos 2.0 [http://www.cbs.dtu.dk/services/NetPhos/]) determined S^{311} as a site for 90-kDa ribosomal S6 kinase (RSK) and PKA. We focused on CLIP-170 regulation by PKA because it is known to phosphorylate numerous MT accessory proteins including p150^{Glued} (Maccioni and Cambiazo, 1995; Gradin et al., 1998; Vaughan et al., 2002; Sengupta et al., 2006).

First, we determined whether PKA directly phosphorylates S^{311} in vitro. Bacterially expressed and purified rat CLIP-170 head (aa 4-354) was phosphorylated by PKA in vitro, and tryptic digests were analyzed by mass spectrometry. The mass of the aa 309-331 tryptic peptide from CLIP-170 treated with PKA differed from the expected mass of the untreated peptide by a phosphate group (80 Da). A collision-induced dissociation spectrum of this peptide showed a loss of H_3PO_4 (98 Da) for the y21 and y22 ions leaving a dehydroalanine at position 311. This confirmed the loss of phosphate at S^{311} upon fragmentation, suggesting that PKA phosphorylates S^{311} (Supplemental Figure 6).

Next, we tested whether PKA induces the interaction between N and C termini of CLIP-170 in cells. PKA activation with forskolin increased the binding of HA-CLIP-170-ΔH to GFP-CLIP-170-H2, whereas the PKA inhibitor H-89 abolished this interaction (Figure 6B). Consistent with this observation, pretreatment of CHO-K1 cells with H-89 resulted in binding of YFP-CLIP-170 to Taxol-stabilized MTs (Figure 6C). Although forskolin alone was not sufficient to induce redistribution of YFP-CLIP-170 at the MT tips (Figure 6C), forskolin in combination with 100 nM OA (a concentration 10 times lower than the IC_{50}) significantly diminished the accumulation of YFP-CLIP-170, restricting its binding to the very distal part of MT ends (Figure 6C). This distribution was similar to that displayed by the phosphomimetic mutant. Treatment with OA at the IC_{50} concentration (1 μM) yielded a similar YFP-CLIP-170 distribution (Figure 6C), suggesting that fully phosphorylated CLIP-170 still binds to MT tips. To confirm the site-specificity of PKA phosphorylation in cells, we performed the above-mentioned treatments with CLIP-170 mutants (Supplemental Figure 7). YFP-CLIP-170 A^{309,311} or YFP-CLIP-170 E^{309,311} mutants were insensitive to activation or inhibition of PKA, confirming the role of PKA in S^{311} phosphorylation in cells. We conclude that PKA phosphorylates CLIP-170 on S^{311} in cells and controls its conformational changes.

DISCUSSION

Regulation of CLIP-170 "On" and "Off" States

Our results demonstrate that CLIP-170 on and off states are modulated by phosphorylation (Figure 7, model). The phosphorylation induces conformational changes in CLIP-170 by increasing the affinity of the N for C terminus, thus resulting in inhibition of protein function. These data are in line with our previous work suggesting that CLIP-170 open and folded back conformations represent active and inactive modes of the protein, respectively (Lansbergen et al., 2004).

Here, we establish the role of five conserved serine residues located in the third serine-rich region in regulating conformational changes as well as CLIP-170 interaction with MTs and p150^{Glued}. Based on our analysis of phosphomimetic and phosphorylation-deficient mutations, which have opposite effects on CLIP-170 affinity for MTs and p150^{Glued}, we extend the evidence for CLIP-170 autoinhibition.

We demonstrated that CLIP-170 can be phosphorylated in cells on multiple residues and that S^{311}, a PKA phosphorylation site, is essential for establishing intramolecular associations. Phosphorylation of S^{309} might have an additive effect but is not sufficient per se to induce CLIP-170 autoinhibition. S^{313}, S^{319}, and S^{320} are potentially important sites for switching CLIP-170 off, although, we did not confirm their phosphorylation in cells. Whether the phosphorylation of these sites might occur during morphogenesis of highly specialized cells such as spermatids, in which CLIP-170 represents an immobile structural component of spermatid manchettes (Akhmanova et al., 2005), or at the onset of mitosis, when CLIP-170 predominantly binds to kinetochores and facilitates the formation of kinetochore–microtubule attachments (Tanenbaum et al., 2006), is to be determined.

Biological Significance of CLIP-170 Phosphorylation

Our data indicate that majority of endogenous CLIP-170 molecules in the cell possess a folded back conformation; therefore, phosphorylation might provide an essential mechanism for the regulation of steady-state "activity" of CLIP-170. This becomes critical in light of our data suggesting that phosphorylation might prevent nonproductive interaction

of CLIP-170 with dynactin–dynein complex. The phosphorylation-deficient mutant of CLIP-170 displays strong binding affinity for p150[Glued], resulting in a significant delay in Golgi reassembly after nocodazole-induced scattering. The loss of CLIP-170 function, however, has no effect on membrane trafficking in our model, and this finding is in agreement with several reports indicating that plus-end localization of p150[Glued] is not required for transport of diverse membrane organelles (Watson and Stephens, 2006; Kim *et al.*, 2007; Lomakin *et al.*, 2009).

CLIP-170 but not p150[Glued] is essential for efficient aggregation of pigment granules, melanosomes, in specialized cells such as *Xenopus* melanophores (Lomakin *et al.*, 2009). It should be noted that aggregation of melanosomes is associated with inhibition of PKA in melatonin-treated cells (Reilein *et al.*, 1998; Rodionov *et al.*, 2003; Kashina and Rodionov, 2005). There is an attractive possibility that dephosphorylation of CLIP-170 might be critical for productive interaction of CLIP-170 with melanosomes at the MT tips, thus ensuring efficient redistribution of thousands of pigment granules in response to extracellular stimuli (Daniolos *et al.*, 1990). In this respect, an accumulation of CLIP-170 at growing MTs also might be important. CLIP-170 rapidly exchanges at the MT tips with diffusion as the rate-limiting factor (Dragestein *et al.*, 2008). The phosphorylation-deficient mutant of CLIP-170 displays much slower turnover at the growing MT ends, suggesting that phosphorylation also might regulate CLIP-170 affinity to the MT lattice (Rickard and Kreis, 1991).

Overall, our data demonstrate that on and off states of CLIP-170 are regulated by phosphorylation-induced autoinhibition. The complex pattern of CLIP-170 phosphorylation in cells might suggest that its function is finely modulated depending on the cellular context.

ACKNOWLEDGMENTS

REFERENCES

Akhmanova, A., *et al.* (2001). Clasps are CLIP-115 and -170 associating proteins involved in the regional regulation of microtubule dynamics in motile fibroblasts. Cell *104*, 923–935.

Akhmanova, A., *et al.* (2005). The microtubule plus-end-tracking protein CLIP-170 associates with the spermatid manchette and is essential for spermatogenesis. Genes Dev. *19*, 2501–2515.

Akhmanova, A., and Steinmetz, M. O. (2008). Tracking the ends: a dynamic protein network controls the fate of microtubule tips. Nat. Rev. Mol. Cell Biol. *9*, 309–322.

Arnal, I., Heichette, C., Diamantopoulos, G. S., and Chretien, D. (2004). CLIP-170/tubulin-curved oligomers coassemble at microtubule ends and promote rescues. Curr. Biol. *14*, 2086–2095.

Beausoleil, S. A., Villen, J., Gerber, S. A., Rush, J., and Gygi, S. P. (2006). A probability-based approach for high-throughput protein phosphorylation analysis and site localization. Nat. Biotechnol. *24*, 1285–1292.

Bieling, P., Kandels-Lewis, S., Telley, I. A., van Dijk, J., Janke, C., and Surrey, T. (2008). CLIP-170 tracks growing microtubule ends by dynamically recognizing composite EB1/tubulin-binding sites. J. Cell Biol. *183*, 1223–1233.

Brummelkamp, T. R., Bernards, R., and Agami, R. (2002). A system for stable expression of short interfering RNAs in mammalian cells. Science *296*, 550–553.

Brunner, D., and Nurse, P. (2000). CLIP170-like tip1p spatially organizes microtubular dynamics in fission yeast. Cell *102*, 695–704.

Busch, K. E., Hayles, J., Nurse, P., and Brunner, D. (2004). Tea2p kinesin is involved in spatial microtubule organization by transporting tip1p on microtubules. Dev. Cell *6*, 831–843.

Carvalho, P., Gupta, M. L., Jr., Hoyt, M. A., and Pellman, D. (2004). Cell cycle control of kinesin-mediated transport of Bik1 (CLIP-170) regulates microtubule stability and dynein activation. Dev. Cell *6*, 815–829.

Choi, J. H., Bertram, P. G., Drenan, R., Carvalho, J., Zhou, H. H., and Zheng, X. F. (2002). The FKBP12-rapamycin-associated protein (FRAP) is a CLIP-170 kinase. EMBO Rep. *3*, 988–994.

Coquelle, F. M., *et al.* (2002). LIS1, CLIP-170's key to the dynein/dynactin pathway. Mol. Cell Biol. *22*, 3089–3102.

Daniolos, A., Lerner, A. B., and Lerner, M. R. (1990). Action of light on frog pigment cells in culture. Pigment Cell Res. *3*, 38–43.

De Zeeuw, C. I., Hoogenraad, C. C., Goedknegt, E., Hertzberg, E., Neubauer, A., Grosveld, F., and Galjart, N. (1997). CLIP-115, a novel brain-specific cytoplasmic linker protein, mediates the localization of dendritic lamellar bodies. Neuron *19*, 1187–1199.

Dragestein, K. A., van Cappellen, W. A., van Haren, J., Tsibidis, G. D., Akhmanova, A., Knoch, T. A., Grosveld, F., and Galjart, N. (2008). Dynamic behavior of GFP-CLIP-170 reveals fast protein turnover on microtubule plus ends. J. Cell Biol. *180*, 729–737.

Dujardin, D., Wacker, U. I., Moreau, A., Schroer, T. A., Rickard, J. E., and De Mey, J. (1998). Evidence for a role of CLIP-170 in the establishment of metaphase chromosome alignment. J. Cell Biol. *141*, 849–862.

Folker, E. S., Baker, B. M., and Goodson, H. V. (2005). Interactions between CLIP-170, tubulin, and microtubules: implications for the mechanism of Clip-170 plus-end tracking behavior. Mol. Biol. Cell *16*, 5373–5384.

Fukata, M., Watanabe, T., Noritake, J., Nakagawa, M., Yamaga, M., Kuroda, S., Matsuura, Y., Iwamatsu, A., Perez, F., and Kaibuchi, K. (2002). Rac1 and Cdc42 capture microtubules through IQGAP1 and CLIP-170. Cell *109*, 873–885.

Goodson, H. V., Skube, S. B., Stalder, R., Valetti, C., Kreis, T. E., Morrison, E. E., and Schroer, T. A. (2003). CLIP-170 interacts with dynactin complex and the APC-binding protein EB1 by different mechanisms. Cell Motil. Cytoskeleton *55*, 156–173.

Gradin, H. M., Larsson, N., Marklund, U., and Gullberg, M. (1998). Regulation of microtubule dynamics by extracellular signals: cAMP-dependent protein kinase switches off the activity of oncoprotein 18 in intact cells. J. Cell Biol. *140*, 131–141.

Gupta, K. K., Paulson, B. A., Folker, E. S., Charlebois, B., Hunt, A. J., and Goodson, H. V. (2009). Minimal plus-end tracking unit of the cytoplasmic linker protein CLIP-170. J. Biol. Chem. *284*, 6735–6742.

Hegeman, A. D., Harms, A. C., Sussman, M. R., Bunner, A. E., and Harper, J. F. (2004). An isotope labeling strategy for quantifying the degree of phosphorylation at multiple sites in proteins. J. Am. Soc. Mass Spectrom. *15*, 647–653.

Hoogenraad, C. C., Akhmanova, A., Grosveld, F., De Zeeuw, C. I., and Galjart, N. (2000). Functional analysis of CLIP-115 and its binding to microtubules. J. Cell Sci. *113*, 2285–2297.

Howard, J., and Hyman, A. A. (2003). Dynamics and mechanics of the microtubule plus end. Nature *422*, 753–758.

Howard, J., and Hyman, A. A. (2007). Microtubule polymerases and depolymerases. Curr. Opin. Cell Biol. *19*, 31–35.

Kashina, A., and Rodionov, V. (2005). Intracellular organelle transport: few motors, many signals. Trends Cell Biol. *15*, 396–398.

Kim, H., Ling, S. C., Rogers, G. C., Kural, C., Selvin, P. R., Rogers, S. L., and Gelfand, V. I. (2007). Microtubule binding by dynactin is required for microtubule organization but not cargo transport. J. Cell Biol. *176*, 641–651.

Komarova, Y. A., Akhmanova, A. S., Kojima, S., Galjart, N., and Borisy, G. G. (2002). Cytoplasmic linker proteins promote microtubule rescue in vivo. J. Cell Biol. *159*, 589–599.

Komarova, Y., Lansbergen, G., Galjart, N., Grosveld, F., Borisy, G. G., and Akhmanova, A. (2005). EB1 and EB3 control CLIP dissociation from the ends of growing microtubules. Mol. Biol. Cell *16*, 5334–5345.

Lansbergen, G., *et al.* (2004). Conformational changes in CLIP-170 regulate its binding to microtubules and dynactin localization. J. Cell Biol. *166*, 1003–1014.

Lewkowicz, E., Herit, F., Le Clainche, C., Bourdoncle, P., Perez, F., and Niedergang, F. (2008). The microtubule-binding protein CLIP-170 coordinates mDia1 and actin reorganization during CR3-mediated phagocytosis. J. Cell Biol. *183*, 1287–1298.

Lomakin, A. J., Semenova, I., Zaliapin, I., Kraikivski, P., Nadezhdina, E., Slepchenko, B. M., Akhmanova, A., and Rodionov, V. (2009). CLIP-170-

dependent capture of membrane organelles by microtubules initiates minus-end directed transport. Dev. Cell 17, 323–333.

Maccioni, R. B., and Cambiazo, V. (1995). Role of microtubule-associated proteins in the control of microtubule assembly. Physiol. Rev. 75, 835–864.

Mimori-Kiyosue, Y., et al. (2005). CLASP1 and CLASP2 bind to EB1 and regulate microtubule plus-end dynamics at the cell cortex. J. Cell Biol. 168, 141–153.

Mishima, M., Maesaki, R., Kasa, M., Watanabe, T., Fukata, M., Kaibuchi, K., and Hakoshima, T. (2007). Structural basis for tubulin recognition by cyto-plasmic linker protein 170 and its autoinhibition. Proc. Natl. Acad. Sci. USA 104, 10346–10351.

Peloquin, J., Komarova, Y., and Borisy, G. (2005). Conjugation of fluorophores to tubulin. Nat. Methods 2, 299–303.

Perez, F., Diamantopoulos, G. S., Stalder, R., and Kreis, T. E. (1999). CLIP-170 highlights growing microtubule ends in vivo. Cell 96, 517–527.

Pierre, P., Scheel, J., Rickard, J. E., and Kreis, T. E. (1992). CLIP-170 links endocytic vesicles to microtubules. Cell 70, 887–900.

Reilein, A. R., Tint, I. S., Peunova, N. I., Enikolopov, G. N., and Gelfand, V. I. (1998). Regulation of organelle movement in melanophores by protein kinase A (PKA), protein kinase C (PKC), and protein phosphatase 2A (PP2A). J. Cell Biol. 142, 803–813.

Rickard, J. E., and Kreis, T. E. (1990). Identification of a novel nucleotide-sensitive microtubule-binding protein in HeLa cells. J. Cell Biol. 110, 1623–1633.

Rickard, J. E., and Kreis, T. E. (1991). Binding of pp170 to microtubules is regulated by phosphorylation. J. Biol. Chem. 266, 17597–17605.

Rodionov, V., Yi, J., Kashina, A., Oladipo, A., and Gross, S. P. (2003). Switching between microtubule- and actin-based transport systems in melanophores is controlled by cAMP levels. Curr. Biol. 13, 1837–1847.

Scheel, J., Pierre, P., Rickard, J. E., Diamantopoulos, G. S., Valetti, C., van der Goot, F. G., Haner, M., Aebi, U., and Kreis, T. E. (1999). Purification and analysis of authentic CLIP-170 and recombinant fragments. J. Biol. Chem. 274, 25883–25891.

Schuyler, S. C., and Pellman, D. (2001). Microtubule "plus-end-tracking pro-teins": the end is just the beginning. Cell 105, 421–424.

Sengupta, A., Grundke-Iqbal, I., and Iqbal, K. (2006). Regulation of phosphor-ylation of tau by protein kinases in rat brain. Neurochem. Res. 31, 1473–1480.

Tai, C. Y., Dujardin, D. L., Faulkner, N. E., and Vallee, R. B. (2002). Role of dynein, dynactin, and CLIP-170 interactions in LIS1 kinetochore function. J. Cell Biol. 156, 959–968.

Tanenbaum, M. E., Galjart, N., van Vugt, M. A., and Medema, R. H. (2006). CLIP-170 facilitates the formation of kinetochore-microtubule attachments. EMBO J. 25, 45–57.

Vaughan, P. S., Miura, P., Henderson, M., Byrne, B., and Vaughan, K. T. (2002). A role for regulated binding of p150(Glued) to microtubule plus ends in organelle transport. J. Cell Biol. 158, 305–319.

Watson, P., and Stephens, D. J. (2006). Microtubule plus-end loading of p150(Glued) is mediated by EB1 and CLIP-170 but is not required for intra-cellular membrane traffic in mammalian cells. J. Cell Sci. 119, 2758–2767.

Weisbrich, A., Honnappa, S., Jaussi, R., Okhrimenko, O., Frey, D., Jelesarov, I., Akhmanova, A., and Steinmetz, M. O. (2007). Structure-function relationship of CAP-Gly domains. Nat. Struct. Mol. Biol. 14, 959–967.

Wieland, G., Orthaus, S., Ohndorf, S., Diekmann, S., and Hemmerich, P. (2004). Functional complementation of human centromere protein A (CENP-A) by Cse4p from Saccharomyces cerevisiae. Mol. Cell Biol. 24, 6620–6630.

Yang, X., Li, H., Liu, X. S., Deng, A., and Liu, X. (2009). Cdc2-mediated phosphorylation of CLIP-170 is essential for its inhibition of centrosome reduplication. J. Biol. Chem. 284, 28775–28782.